Inertia forces on conductor arrays in a jacket model in regular waves

H. Santo[1] (harrif.santo@eng.ox.ac.uk), P. H. Taylor[1], A. H. Day[2]

[1] Department of Engineering Science, University of Oxford,
Parks Road, Oxford OX1 3PJ, UK

[2] Department of Naval Architecture and Marine Engineering, University of Strathclyde,
Henry Dyer Building, 100 Montrose Street, Glasgow G4 0LZ, UK

- A wave phase-based force decomposition allows inertia and drag forces to be separated, we focus here on the inertia force on conductor arrays (closely spaced vertical cylinders).
- The measured inertia force coefficient of the 1st harmonic force component is very close to 2 for waves both with and without current. For waves without current, the coefficient of the 2nd harmonic force is within 10% of 5/4, the corresponding term in the FNV model. For waves with current, the coefficient of the 2nd harmonic force increases noticeably as the current increases.
- The effect of conductor spacing is investigated numerically. For the jacket end-on, even when the closest conductors touch, the change in effective C_M ~ –5%. In contrast for broadside where the spacing is effectively closer, the change is ~ +45%.

1. Introduction

The hydrodynamic loading on space-frame offshore structures has been re-visited recently by Taylor et al. (2013) and Santo et al. (2014) because of the growing interest in the oil industry in the re-assessment of ageing offshore infrastructure. For space-frame structures, the Morison equation has been used universally for design; this describes the total hydrodynamic force as a sum of drag and inertia forces (Morison et al. 1950). Typically the most extreme fluid-loading regime is dominated by drag; hence the study of Taylor et al. (2013) was focused on the behaviour of the drag term. For regular waves with in-line current, the drag term has been shown to be overestimated by the Morison equation because of the occurrence of additional blockage which further reduces the mean flow on the structure. This additional flow reduction is in addition to the standard industry practice of including a simple current blockage factor as documented in API (American Petroleum Institute 2000).

Here we report observations on what we assume are the linear and nonlinear potential flow (inertia) forces in recent experiments on a jacket model. We compare the force coefficients for the first three frequency harmonics of the measured force (those components out of phase with the wave crests) with the FNV-force equation from Faltinsen et al. (1995), see also Malenica & Molin (1995), for the total horizontal load on vertical cylinders. This allows us to investigate the contribution of the linear and non-linear components of the total inertia force. Previous experimental studies have been carried out by Chaplin et al. (1997) and others to look at the force on a single or a few vertical cylinders. Here, we also look at the force on arrays of cylinders representing conductors, examining the interaction effects on the linear inertia term on arrays of cylinders for different wave directions.

2. Experimental set up & data analysis

A series of experiments were conducted in the towing tank in the Kelvin Hydrodynamics Laboratory of Strathclyde University, Glasgow, as an extension of previous work to verify the improved fluid loading recipe on a scaled jacket model, as well as to formulate an appropriate current blockage recipe for irregular waves. A 1:80 jacket model was constructed from stainless steel (figure 1 shows the model); this resembles a typical second generation North Sea jacket 4-leg structure. The jacket was hung below the carriage, such that the still-water submerged height of the jacket was 1.45 m. The carriage was moved at constant speed along the tank to simulate uniform current, and the model was exposed to regular waves of various wave heights with a fixed wave period of 1.4 sec on a water depth of 2.1 m. The jacket was mounted in such a way that the total horizontal reaction due to the hydrodynamic load was measured directly by a force transducer. A wave gauge was mounted on the carriage between the jacket model and the side of the tank to provide phase information of the undisturbed incoming waves. A combination of 5 different heights of regular wave and 3 towing speeds (current) were tested.

The jacket model is tapered when viewed end-on and rectangular broadside (see figure 1 for the plan view). Also shown are the conductor support frames and the arrangement of the conductor arrays (vertical closely spaced uniform cylinders). The conductor support frames, made of square hollow members instead of cylindrical members, were supported on the horizontal bracings at end-on instead of extending from the jacket legs (as commonly found in actual offshore jackets) to ease the fabrication process. The conductors in the jacket model were designed to be removed

easily from the carriage so a combination of cases with and without conductors for the same wave loading direction is possible. For hydrodynamic loading in the broadside direction, there are rows of four conductor tubes side-by-side orthogonal to the flow direction. In contrast, for end-on direction, there are rows of only two conductor tubes. Interaction effects are expected in the inertia forces of broadside and end-on, both with conductors. In total, three configurations of the jacket model were tested: broadside with conductors, end-on with conductors, and end-on without conductors. No cases of broadside without conductors were tested.

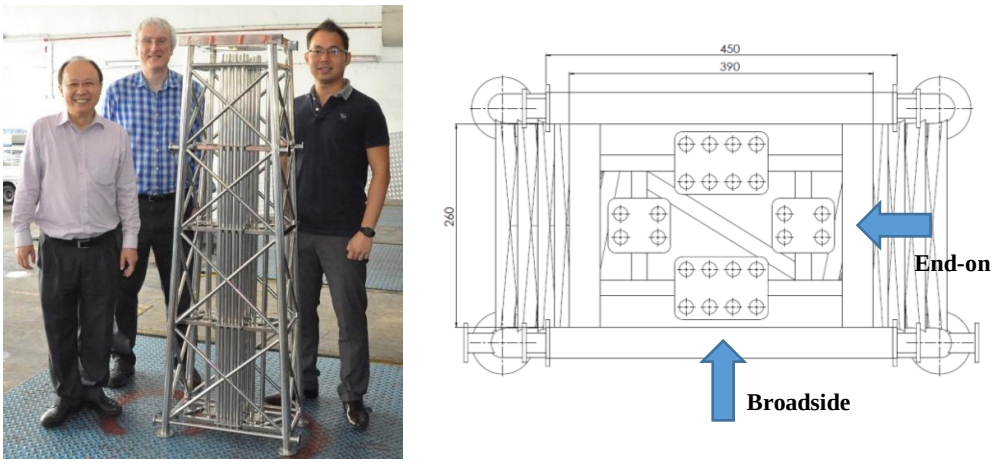

Figure 1: (Left) 3D view of the jacket model and (Right) plan view of the model showing the arrangement of conductor arrays.

The total measured forces were decomposed into a sum of drag and inertia forces following the decomposition method outlined in Santo et al. (2014). The phase information of the wave is required, and the key assumption made is force symmetry around the wave crest/horizontal velocity peak. The total force was extracted after the starting transients when the force is periodic in time, and phase-averaged (cycle-by-cycle) over a record of 10 – 20 wave cycles before the decomposition. That part of the total force in-phase with the wave velocity is assumed to be drag, the remainder that is out of phase is assumed to arise from potential flow load components, with the linear part (in both frequency and wave amplitude) being the Morison inertia term. Figure 2 (left) shows a plot of the decomposition for 0.24 m regular waves in the end-on direction with no current. The drag force will be compared with the new blockage theory (Taylor et al. 2013) elsewhere. Here, we focus on the inertia force and its harmonics (Fig. 2 top right).

3. Inertia force on conductor arrays in end-on

To investigate the experimentally measured inertia force, we chose to look at the measured inertia force on the conductor arrays only, by subtracting the inertia force on the model without conductors for waves end-on from the inertia force for the same model tested with conductors. Thus, the effects of legs, braces, and other cylindrical members that are non-orthogonal to the flow as well as square hollow members which have different C_M values should be removed. This will allow a cleaner investigation: all the conductor tubes run vertically the full height of the jacket, forming an array of uniform, closely spaced cylinders of diameter 1.6 cm.

We fit the measured inertia forces using the MATLAB curve fitting toolbox. The phase of the wave is obtained from the wave gauge signal, so the phases of both drag and inertia terms are known. We take a -90° phase shift for the harmonic term of the inertia force relative to the wave crest and obtain force coefficients of the 1st up to 3rd harmonic terms in frequency. We compare the force fits with those of the nonlinear potential flow FNV force on a single uniform vertical surface-piercing cylinder (Faltinsen et al. 1995): with $\eta = A\,cos\,\omega t$ as the linear part of the wave profile, the FNV force is $F_{Inertia}/\pi r^2 = -2\rho g A\,sin\omega t - 5/4\rho g A^2 k\,sin2\omega t - 2\rho g A^3 k^2\,sin3\omega t$, where r is the cylinder radius and the other symbols have their usual meanings. The FNV force model assumes the linear inertia coefficient $C_M = 2$ and contains force coefficients of 1.25 and 2 for the 2nd and 3rd harmonic terms, respectively.

For waves with no current, the mean value of force coefficients on the conductor array are 2.08 (1st harmonic), 1.35 (2nd harmonic) and 6.02 (3rd harmonic). The first two harmonics agree reasonably well with the predictions from the FNV model, the 3rd harmonic term differs considerably but the signal is small and noisy. We also believe that there may be some small phase leakage across from the drag term for the 3rd frequency harmonic. In calculating the force coefficients, the effect of finite water depth was taken into account (a 5% correction to deep water kinematics assumption). Figure 2 (right) shows the forces on the conductor arrays for 0.24 m regular waves with no current.

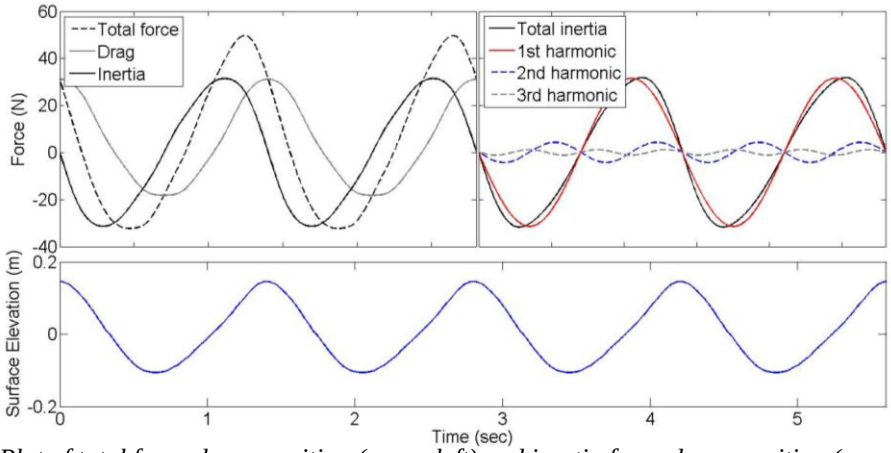

Figure 2: Plot of total force decomposition (upper left) and inertia force decomposition (upper right), both for 0.24 m regular waves with no current. The bottom figure shows the surface elevation.

The current is simulated by towing the jacket model along the tank, so the wave kinematics are unaffected by the current, but the encounter rate of the model with the waves changes. Hence, in a moving frame of reference (moving with jacket), the wave horizontal velocity can be written as: $U_{Wave} \sim \omega A \cos[(\omega + U_C k)t - kx]$. Therefore, the linear inertia term contains the encounter frequency due to current: $\partial U_{Wave}/\partial t \sim -\omega(\omega + U_C k)A \sin[(\omega + U_C k)t - kx]$ and as a result, the total linear contribution in the inertia force with $C_M = 2$ can be expressed as $\sim(2 \cdot \partial U_{Wave}/\partial t + U_C \, \partial U_{Wave}/\partial x)$. When integrated over the height of the model to mean sea level, this yields a factor of $-2\left(1 + \frac{U_C}{2C_\emptyset}\right)\times$, where $C_\emptyset = \omega/k$ is the phase speed of the wave. The additional term $(U_C/2C_\emptyset)$ arises from the current contribution to the 1st harmonic term. We assume that the rest of the FNV-model is unaltered. Clearly for the case with current, the 2nd order term in wave amplitude could be expected to be generalised to have current × wave terms contributing to the 1st harmonic component. The 3rd order term for waves with no current would be expected to produce 1st and 2nd harmonic contributions with the current present. Unfortunately we know of no extension of the FNV-model to account for the effect of current on the 2nd and higher harmonic terms.

Figure 3 shows the values of the force coefficients for all cases with and without current. For the 1st harmonic term (left), the measured C_M values are all close to the theoretical $C_M = 2$ (solid line). For the coefficient of the 2nd harmonic term (right), with the theoretical FNV value of 5/4 (solid line), the experimental mean of 1.35 (for no current – dashed black line) is quite close. As the current speed is increased the 2nd order coefficients also increase, from 1.35 to 1.92 (for 0.14 m/s current – red line) and 2.18 (for 0.28 m/s current – blue line). We suspect the increase is associated to the current but have no model to account for it.

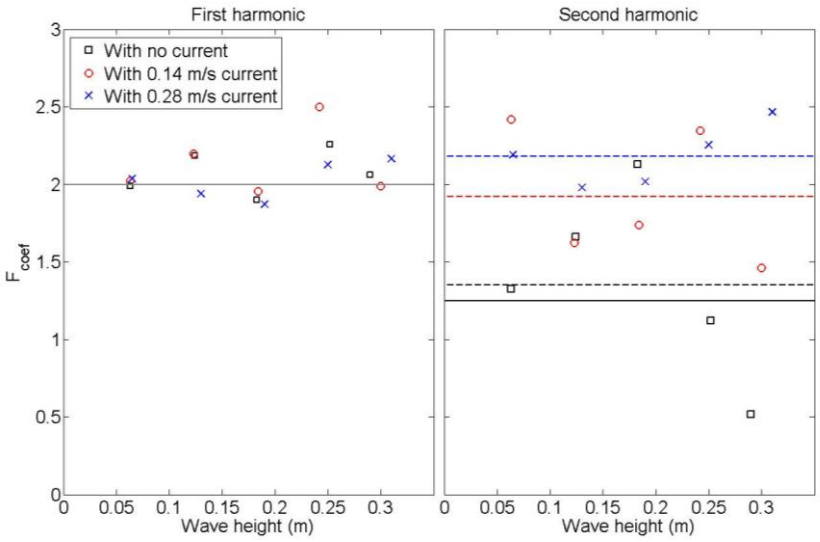

4. Interactions within conductor arrays

The effect of conductor arrays in regular waves is known to induce (wake) shielding, which can be captured with a reduced drag coefficient in the Morison equation, and either the full current blockage model from Taylor et al. (2013) or the API standard (figure C.3.2-4) can be used to account for such an effect. The effect on the inertia term however, is less clear.

Figure 3: Plot of force coefficient variations with wave height and current speed.

From the measured inertia forces, we obtain C_M of about 2.0 for the conductor array in the end-on orientation, suggesting that the experimental evidence is compatible with potential flow theory prediction. What about the same structure in the broadside orientation? Would the arrangement of the conductor tubes end-on vs. broadside matter in terms of C_M? We have no experimental data as yet, but a simple potential flow model (Walker & Eatock Taylor 2005), based on Linton & Evans (1990) analysis of multiple cylinders, was used to examine this.

For the arrangement of conductor arrays we have for the jacket model, the smallest spacing (centre to centre) to diameter ratio of conductor tubes (S/D) is 1.7 for both end-on and broadside directions. From the potential flow model, the net effective C_M for end-on is 0.96× the undisturbed C_M, for broadside is 1.07×. The increase/decrease in C_M is associated with the interaction effects of neighbouring cylinders. For broadside, there are four rows of four cylinders, while for end-on there are only rows of two cylinders. Whilst for the experimental configuration there are only small perturbations away from the undisturbed values, it is interesting to ask how much closer would the conductor tubes have to be to produce large changes in C_M?

Figure 4 shows the variation of force coefficients for end-on and broadside. The S/D ratio was adjusted by increasing/decreasing the diameter of the conductor tubes while keeping their centres fixed, with $S/D = 1$ being the limit when the closest conductors touch. The interaction effect for waves end-on is small; the force coefficient decreases as S/D reduces up to the point when the two conductors at the first two and last two rows in the end-on direction are about to touch. The interaction effect is larger in the broadside direction, where the increase in C_M is now up to 45% in the limit when the conductors in the rows of four cylinders are touching. Whilst closely-spaced conductor arrays are known to reduce the drag term in the Morison equation due to blockage, in contrast the linear inertia term could increase, depending on the arrangement of the conductor arrays. Any increase in the inertia term is obviously relevant to fatigue prediction.

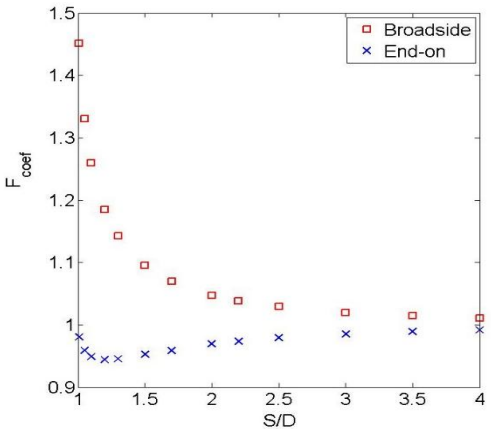

Figure 4: Plot of force coefficients versus S/D for end-on and broadside.

Acknowledgements:

The authors are grateful to Prof. Y.S. Choo of the National University of Singapore and Prof. R. Eatock Taylor of University of Oxford for their help with this work.

References

American Petroleum Institute, 2000. Recommended practice for planning, designing, and constructing fixed offshore platforms: working stress design. API RP2A-WSD 21st Edition with Errata and Supplements.

Chaplin, J. R., Rainey, R. C. T., & Yemm, R. W., 1997. Ringing of a vertical cylinder in waves. *J. Fluid Mech.* **350**, 119–147.

Faltinsen, O. M., Newman, J.N., & Vinje, T., 1995. Nonlinear wave loads on a slender vertical cylinder. *J. Fluid Mech*. **289**, 179–198.

Linton, C. M., & Evans, D. V., 1990. The interaction of waves with arrays of vertical circular cylinders. *J. Fluid Mech.* **215**, 549–569.

Malenica, S., & Molin, B., 1995. Third-harmonic wave diffraction by a vertical cylinder. *J. Fluid Mech.* **302**, 203–229.

Morison, J. R., Johnson, J. W., & Schaaf, S. A., 1950. The force exerted by surface waves on piles. *J. Petroleum Technology*, ***2***(5), 149–154.

Taylor, P. H., Santo, H., & Choo, Y. S., 2013. Current blockage: Reduced Morison forces on space frame structures with high hydrodynamic area, and in regular waves and current. *Ocean Eng.* **57**, 11–24.

Santo, H., Taylor, P. H., Williamson, C. H. K., & Choo, Y. S., 2014. Current blockage experiments: Force time histories on obstacle arrays in combined steady and oscillatory motion. *J. Fluid Mech*. **739**, 143–178.

Walker, D. A. G., & Eatock Taylor, R., 2005. Wave diffraction from linear arrays of cylinders. *Ocean Eng*, ***32***, 2053–2078.